NASA TECHNICAL MEMORANDUM

NASA TM X-62,252

NASA TM X-62,252

AERODYNAMIC CHARACTERISTICS OF A SWEPT AUGMENTOR WING

David G. Koenig and Michael D. Falarski

Ames Research Center
and
U.S. Army Air Mobility R&D Laboratory
Moffett Field, Calif. 94035

October 1972

AERODYNAMIC CHARACTERISTICS OF A SWEPT AUGMENTOR WING

By David G. Koenig
NASA Ames Research Center

and

Michael D. Falarski
U.S. Army Air Mobility R&D Laboratory

SUMMARY

A brief outline of augmentor wing research sponsored by Ames Research Center is presented and is followed by a discussion of large-scale wind-tunnel test results for a swept augmentor wing configuration. The results showed that the augmentor wing could be applied to high-speed swept wing designs with little adverse effect on either the basic performance of the augmentor or the longitudinal characteristics, including maximum lift and stall. Three lateral control devices were shown to be effective and ground effect was measured for several complete aircraft configurations.

INTRODUCTION

As part of continuing research and development of the augmentor wing powered high-lift systems, tests have been made recently on a swept augmentor wing. Although the augmentor performed well on simple unswept wing planforms, there were significant questions concerning the adverse effects of sweep and taper ratio on augmentor wing performance. Design studies have shown that angles of sweep up to 25^{o} would be required in order to maintain sufficient wing thickness to enclose the required ducting as well as to maintain the required cruise Mach numbers for augmentor wing aircraft.

Areas which could be adversely affected by this sweep are as follows: Augmentor performance – particularly at airspeed – could be affected by sweeping the augmentor inlet with respect to the local flow coming from the wing upper surface. Aircraft performance near 1g flight would be affected by adverse effects on basic forces and moments in view of previous experience in the application of other high-lift devices to swept wings. Characteristics at high angle of attack such as maximum lift and stall could be adversely affected by sweep. And, finally, lateral stability and control and ground effect are items which must be documented for use in design studies.

The wind-tunnel test program using a large-scale swept wing model was designed to answer questions in the areas just mentioned. Results will be summarized in this paper following a brief outline of augmentor wing research at Ames Research Center.

NOTATION

b	wing span, m (ft)
c	wing chord, m (ft)
$\bar{c}$	mean aerodynamic chord, m (ft)
C_D	drag coefficient, $\frac{\text{Drag}}{qS}$
C_{J_I}	total isentropic jet thrust coefficient, including augmentor, aileron BLC, and fuselage BLC, $\frac{F_I}{qS}$
C_L	lift coefficient, $\frac{\text{Lift}}{qS}$
C_l	rolling-moment coefficient, $\frac{\text{Rolling moment}}{qSb}$
C_m	pitching-moment coefficient, $\frac{\text{Pitching moment}}{qS\bar{c}}$
C_n	yawing-moment coefficient, $\frac{\text{Yawing moment}}{qSb}$
C_p	pressure coefficient, $\frac{p_l - p_\infty}{q}$
F	force of augmentor measured on static test, N (lb)
F_I	isentropic jet thrust, N (lb)
F_{nozzle}	force of primary nozzle, N (lb)
h	distance from ground to model wing chord plane at $\alpha = 0^o$, N (ft)
p_l	wing surface static pressure, N/m^2 (psf)
p_∞	free-stream static pressure, N/m^2 (psf)
q	free-stream dynamic pressure, N/m^2 (psf)
S	wing area, m^2 (ft^2)

T/W	ratio of total static engine thrust to aircraft weight
α	model angle of attack, deg
β	angle of sideslip, deg
δ_a	aileron deflection, deg
δ_f	augmentor deflection, augmentor centerline rotation from wing chord plane, deg
δ_{th}	engine residual thrust nozzle rotation, 0 when nozzle is parallel to wing chord plane, deg

BACKGROUND

The augmentor wing has been studied as a powered high-lift device which can be integrated with the aircraft propulsion system to improve the landing and takeoff characteristics of STOL aircraft. Work was started with unswept wing configurations in order to simplify the study of augmentor performance at forward speed. This was also a promising configuration which could result in a flight-test vehicle that could be built economically. A sketch of one of the more recent unswept-augmentor-wing-model configurations is shown in figure 1. Results of wind-tunnel tests on these configurations are presented in references 1 and 2. It was found that the aerodynamics of the configuration were good, particularly the longitudinal stability and control characteristics.

The augmentor wing was then chosen as the powered high-lift system for use on the NASA flight research vehicle. This aircraft is being flight tested, and initial flight-test results will be reported on by Hervey C. Quigley and Richard F. Vomaski.

Work on advanced augmentor wing configurations has been continuing in order to improve augmentor performance and reduce noise of the augmentor wing. These subjects are also discussed in subsequent papers. Advanced augmentor wing concepts are being integrated into aircraft design studies and should be sufficiently generalized to help in the direction of future research and development. Some initial results in this effort are presented in references 3 to 6.

A significant part of this work is the study of the cruise augmentor wing. This is basically a thrust augmentor used as a propulsion device for aircraft at cruise. Two cruise augmentor wing programs are being sponsored by Ames Research Center. One is included in a contract with The Boeing Company and the other is a joint effort of the

United States and Canada. Each program has a different approach, but either design could lead to reduced weight and simplification of augmentor-wing-aircraft lift-propulsion systems.

The remainder of this paper summarizes results of recent tests in the Ames 40- by 80-foot wind tunnel. During the last 2 years, tests in and out of ground effect were made in a joint effort between the United States and Canada. The test data for these tests are presented in references 7, 8, and 9 and are summarized in the following discussion.

MODEL AND TEST DESCRIPTION

Figure 2 shows the model planform superimposed on the configuration used in a previous unswept wing test. The wing was swept 27.5° and had a slightly larger aspect ratio than the unswept wing. The wing had a taper ratio of 0.3 and an average section thickness of 0.115 compared with 0.4 and 0.16, respectively, for the unswept wing. As with the unswept wing the model had blown ailerons, used a full-span slat for leading-edge stall control, and was equipped with provisions for BLC across the top of the fuselage to control root stall. Further description of the model is presented in references 7, 8, and 9.

Photographs of the models are shown in figures 3, 4, and 5. Figures 3 and 5 show the model equipped with 4 JT15D powered nacelles to simulate unvectored residual thrust of the engine. The model is shown in figure 4 equipped with J85 nacelles. The nozzles for each of these nacelles swiveled from thrusting back parallel with the nacelle centerline to 30° forward of vertical. For the out-of-ground-effect tests the model was installed near the center of the wind-tunnel test section. The model was tested near the floor of the wind tunnel to simulate the effect of ground as shown in figures 4 and 5.

A comparison of the augmentor configuration with a previous configuration used on the unswept wing is shown in figure 6. The primary difference was the elimination of the slot on the flap. Bench tests of 2D models made prior to installation of the augmentor model indicated that augmentation ratios F/F_I were decreased from a maximum of 1.39 to 1.37 by eliminating this slot.

RESULTS AND DISCUSSION

Augmentor Performance

Prior to the wind-tunnel tests, the augmentation of the fully assembled augmentor was measured with the model on a static test stand. The results are summarized in figure 7 and are presented in more detail in reference 8. Augmentation ratio shown is the ratio of augmentor measured thrust to the nozzle thrust measured with the augmentor

removed. The maximum values of augmentation ratio of 1.43 and 1.33 for the 2D and large-scale model, respectively, compare well when it is considered that no attempt was made to optimize the augmentor after it was installed on the large-scale model. This comparison between the bench tests and complete model static tests was similar to corresponding comparisons for the unswept model, and it can therefore be concluded that there were no major adverse effects of sweep on static augmentor performance. Preliminary analysis of augmentor performance at forward speed indicated that here no performance was not adversely affected by sweep. Further discussion of the augmentor performance at forward speed is included in paper no. 8 by Thomas N. Aiken.

Longitudinal Characteristics

A comparison of two sets of basic data for the unswept and swept wing configurations is presented in figure 8 for the models with tail off. The ailerons were deflected 45° and 30° for the unswept and swept wings, respectively, the augmentor flap was 50°, and the jet coefficient was 0.8. It is evident that the lift and drag characteristics are similar, with the lift-curve slope and maximum lift the same and the slope of the drag curve being of the same shape. A comparison of the moment data shows that both curves are close to linear and if the moment center for the swept wing model were moved back $0.07\bar{c}$ the two sets of moment data could be superimposed.

The effects of sweep on lift as functions of power and flap deflection are shown in figures 9 and 10 for zero angle of attack as well as maximum lift. The flap lift increments as well as the maximum lift obtained for the swept wing are seen to bracket the values measured for the unswept wing; thus, the effects of power on the lift were the same for the two models. One significant difference appeared in maximum lift (fig. 10); values decreased for the unswept wing as flap deflection increased and remained about the same for the swept wing.

The basic stalling characteristics were different from those of the unswept wing for some wing configurations in that the swept wing generally stalled first at the wing tips whereas the unswept wing generally stalled at the root and fuselage blowing boundary-layer control improved maximum lift for that case (see ref. 2). For the swept wing the effect of symmetric aileron deflection on stall is shown in figure 11 for the landing flap setting $(\delta_f = 70^{\circ})$. The C_{m_α} curves in the upper portion of the figure show pitch-up occurred for the $\delta_a = 30^{\circ}$ and 45° settings. The tendency to pitch up was eliminated up to 32° angle of attack by reducing the aileron droop to 15°. The reason for this is shown by the variation with spanwise location of pressure coefficient on the wing at 0.07c which may be used as a qualitative spanwise load distribution along the wing. The data show a loss in loading at the wing tip and a slight gain in lift at the root. Tendency to pitch up or an adverse stalling characteristic can therefore be reduced by undrooping the

ailerons. As may be seen from the lift data of references 7 and 8, reducing δ_a from 45^o to 15^o reduces $C_{L_{max}}$ by only 0.25.

During the investigations of references 7 and 8, three tail heights were considered for the tail lengths indicated in figure 2. The heights ranged from the extended wing chord plane to $1.4\bar{c}$ above the chord plane. Downwash data were obtained for all three tail positions and tail-on force and moment data are available for the two higher positions. For both of these positions, the stability and control characteristics of the complete aircraft configurations were excellent. As an example, the effect of power on trim is shown in figure 12 for a moment center located at 35 percent chord. The data are chosen for trim lift values of 3.5 and 5.2 for the takeoff and landing flap deflections, respectively, for the condition of 1g flight. As shown, the effect of power was slight for values of T/W of 0.3 and 0.4 and, although not shown, this conclusion is valid for a much larger range of T/W. Also, for the lift range shown, static stability was not influenced greatly by power.

During the tests reported in references 8 and 9, nacelle-wing interference effects were measured, particularly with the powered nacelle configurations shown in figures 4 and 5. In augmentor wing designs, between 40 and 80 percent of the engine thrust is ducted to the augmentor and the remainder is exhausted under the wing. The nacelle-wing interference effects were measured over a thrust range representing these distributions, or thrust splits, and typical results are shown in figure 13 for the four-nacelle configuration with no thrust deflection. The lift and drag values for the takeoff flap setting $(\delta_f = 40^o)$ are presented as functions of augmentor jet thrust C_{J_I} for nacelles off and two thrust splits. The lift and drag coefficients are those resulting after the gross engine thrust has been subtracted. For the higher values of C_{J_I}, the lift for the 60-40 (engine-augmentor) split was 11 percent below the nacelle-off values but a significant portion of this was also measured for the 33-67 split. A split of 25-75 is being seriously considered for some current augmentor wing designs, and for these the adverse effects of both nacelle and residual thrust could probably be considered small. It is believed that adverse effects of residual thrust could be further reduced by slight downward deflection of the jet.

Lateral Characteristics

Lateral stability and control characteristics of the swept augmentor wing model are presented in references 7 and 8. It was shown that both C_{l_β} and C_{n_β} were linear with augmentor thrust and comparable to those of wings equipped with other powered high-lift systems. The lateral control methods investigated proved to be effective, and control options are summarized in figure 14. The data are presented in terms of rolling-moment and yawing-moment increment obtained while one side of each control is cycled. The values were found to be additive except where the aileron is moved together with the spoiler

of the same side since the spoiler reduced the effectiveness of the aileron. An interesting combination of the devices would be the use of the spoilers in conjunction with the augmentor throttling for a fixed symmetrical aileron droop where, as shown by the yawing-moment data, the yawing-moment inputs would tend to cancel and to produce little or no yawing moment due to roll control.

Ground Effect

The ground effect of the model was measured by using the wind-tunnel test-section floor as a fixed ground board with the model installed as shown in figures 4 and 5. Results of the measurements are shown in figures 15 and 16 for the cases of the basic wing and two nacelles installed (configuration of fig. 4), respectively. The lift data are presented for constant angle of attack which represents an aircraft touchdown attitude, and the drag data are shown for a typical approach lift value. The measurements showed that below a value of $C_{J_I} = 0.6$, ground effect was negligible. For values of C_{J_I} above 0.6, the adverse effect on lift increased with C_{J_I} to a value representing a 10-percent reduction in lift. The ground effect on drag for a constant lift coefficient was found to be negligible. It should be noted that these effects were due to reducing ground height $1.34\bar{c}$ which would be approximately wheel height at touchdown.

CONCLUDING REMARKS

In summary, it was found that the augmentor wing could be applied to a high-speed swept wing configuration and result in favorable longitudinal and lateral characteristics. There were found to be no major adverse effects of sweep on augmentation ratio or on basic lift, drag, and moment characteristics; maximum lift and the stall were mild but could be controlled by proper choice of symmetrical aileron droop.

Investigations of the lateral characteristics of the swept augmentor wing indicated that three controls were effective and a system was possible having no yawing-moment input.

Ground effect measurements showed a small adverse effect on lift when ground height was reduced to 1.34 chords or wheel height.

REFERENCES

1. Koenig, David G.; Corsiglia, Victor R.; and Morelli, Joseph P.: Aerodynamic Characteristics of a Large-Scale Model With an Unswept Wing and Augmented Jet Flap. NASA TN D-4610, 1968.

2. Cook, Anthony M.; and Aiken, Thomas N.: Low-Speed Aerodynamic Characteristics of a Large-Scale STOL Transport Model With an Augmented Jet Flap. NASA TM X-62,017, 1971.

3. O'Keefe, J. V.; and Kelley, G. S.: Design Integration and Noise Studies for Jet STOL Aircraft. Vol. I – Program Summary. D6-40552-1 (Contract NAS2-6344), Boeing Co., May 1972. (Available as NASA CR-114471.)

4. Roepcke, F. A.; and Kelley, G. S.: Design Integration and Noise Studies for Jet STOL Aircraft. Vol. II – System Design and Evaluation Studies. D6-40552-2 (Contract NAS2-6344), Boeing Co., May 1972. (Available as NASA CR-114472.)

5. Campbell, J. M.; Lawrence, R. L.; and O'Keefe, J. V.: Design Integration and Noise Studies for Jet STOL Aircraft. Vol. III – Static Test Program. D6-40552-3 (Contract NAS2-6344), Boeing Co., May 1972. (Available as NASA CR-114473.)

6. Wang, T.; Wright, F.; and Mahal, A.: Design Integration and Noise Studies for Jet STOL Aircraft. Vol. IV – Wind Tunnel Test Program. D6-40552-4 (Contract NAS2-6344), Boeing Co., May 1972. (Available as NASA CR-114474.)

7. Falarski, Michael D.; and Koenig, David G.: Aerodynamic Characteristics of a Large-Scale Model With a Swept Wing and Augmented Jet Flap. NASA TM X-62,029, 1971.

8. Falarski, Michael D.; and Koenig, David G.: Longitudinal and Lateral Stability and Control Characteristics of a Large-Scale Model With a Swept Wing and Augmented Jet Flap. NASA TM X-62,145, 1972.

9. Falarski, Michael D.; and Koenig, David G.: Longitudinal Aerodynamic Characteristics of a Large-Scale Model With a Swept Wing and Augmented Jet Flap in Ground Effect. NASA TM X-62,174, 1972.

UNSWEPT WING MODEL

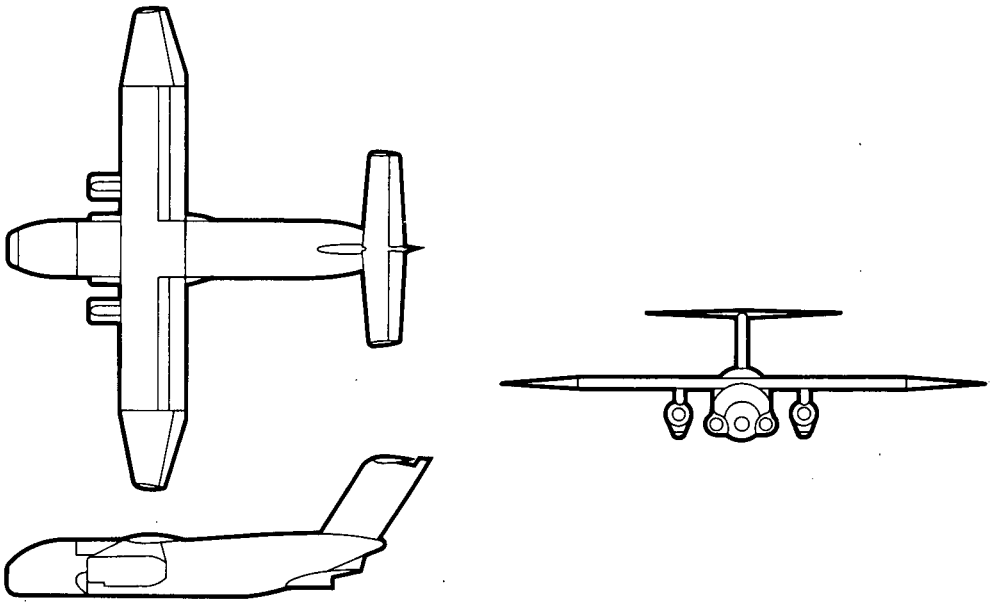

Figure 1

COMPARISON OF SWEPT AND UNSWEPT WING MODEL CONFIGURATIONS

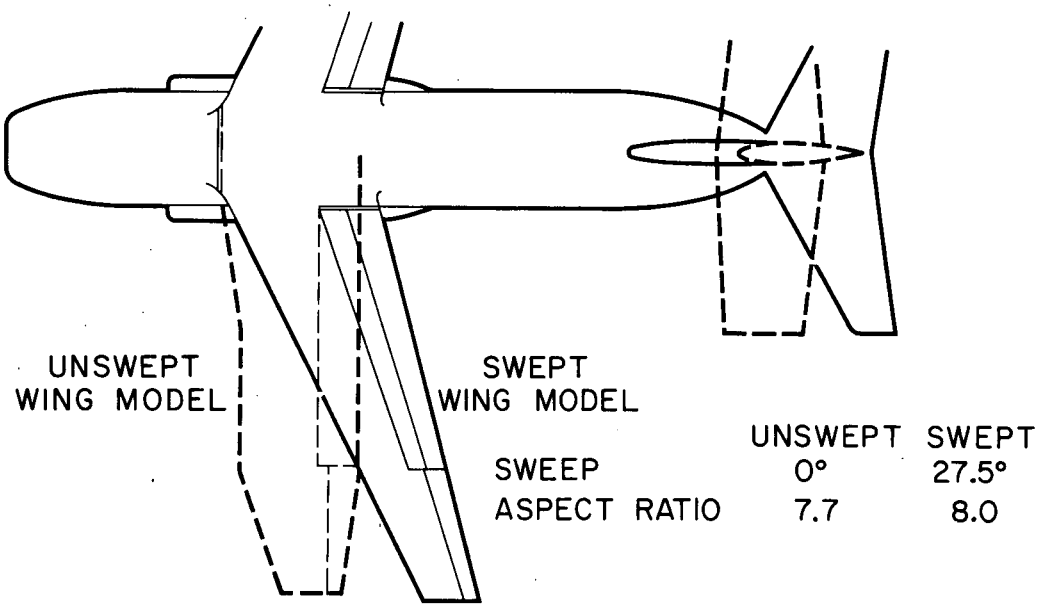

Figure 2

SWEPT WING MODEL INSTALLED IN THE
40-BY 80-FOOT WIND TUNNEL

Figure 3

AUGMENTOR WING MODEL INSTALLED IN WIND
TUNNEL FOR GROUND EFFECT TESTS

J85 NACELLES

Figure 4

AUGMENTOR WING MODEL INSTALLED IN WIND TUNNEL FOR GROUND EFFECT TESTS

JT15D NACELLES

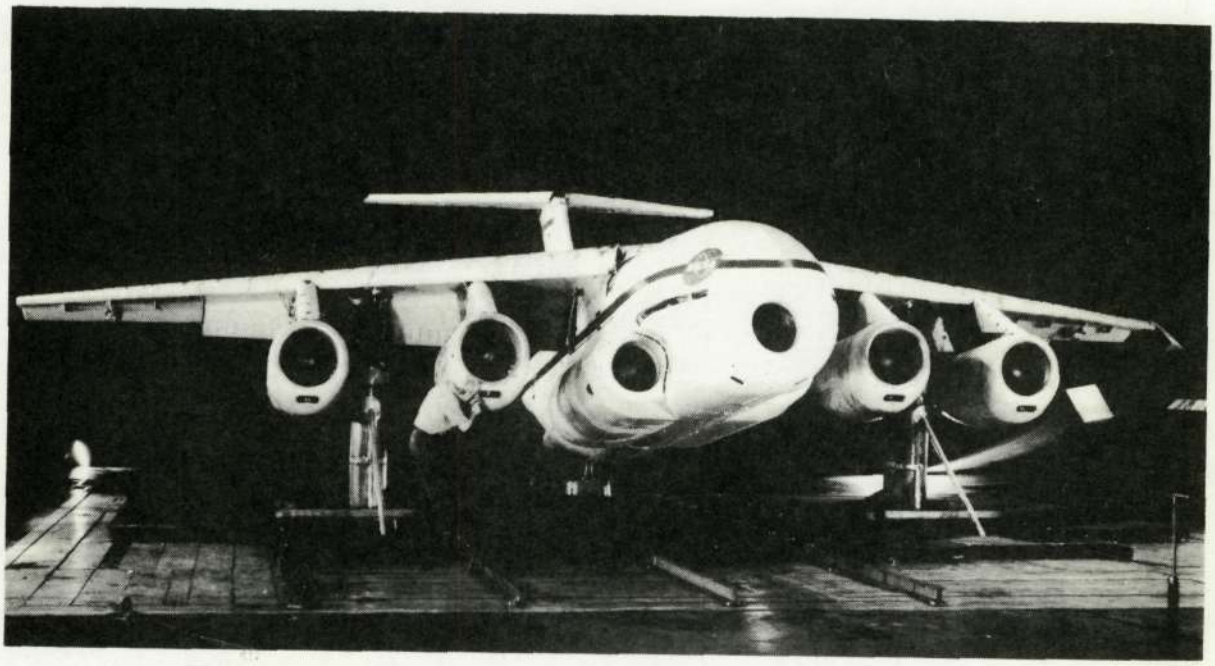

Figure 5

STREAMWISE SECTION OF AUGMENTOR FLAP

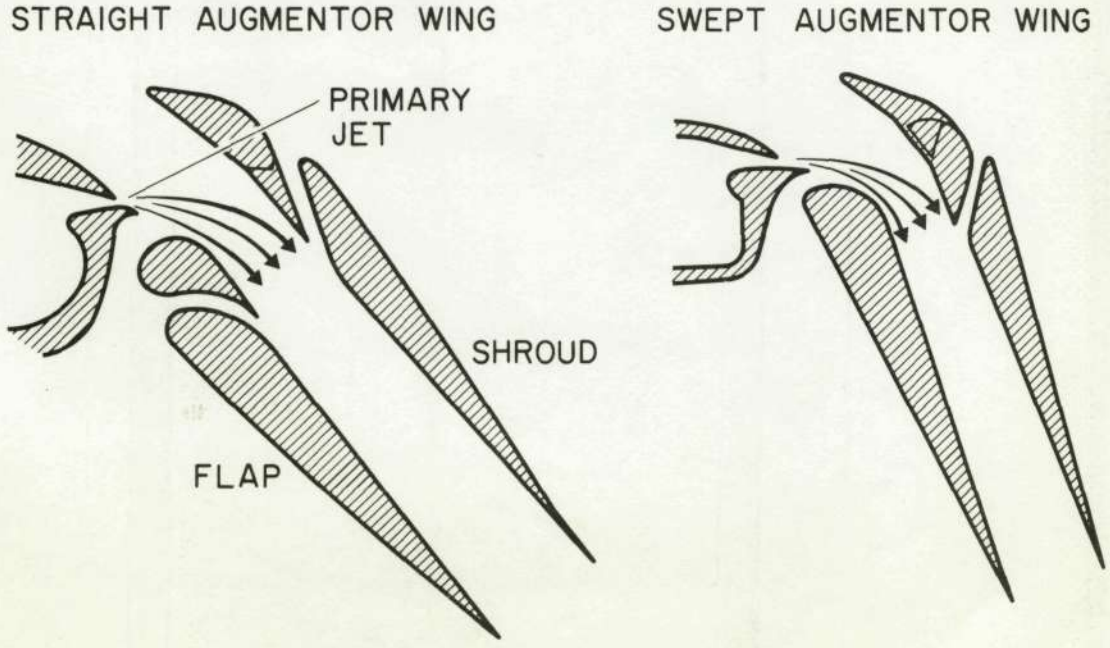

Figure 6

AUGMENTOR STATIC PERFORMANCE FOR
SWEPT WING

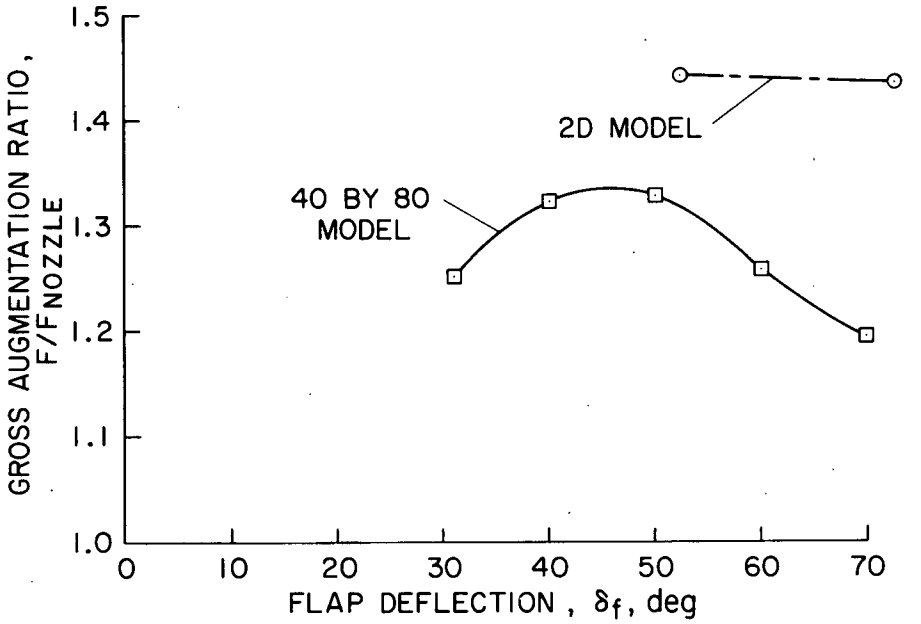

Figure 7

UNSWEPT AND SWEPT WING COMPARISON
LONGITUDINAL CHARACTERISTICS

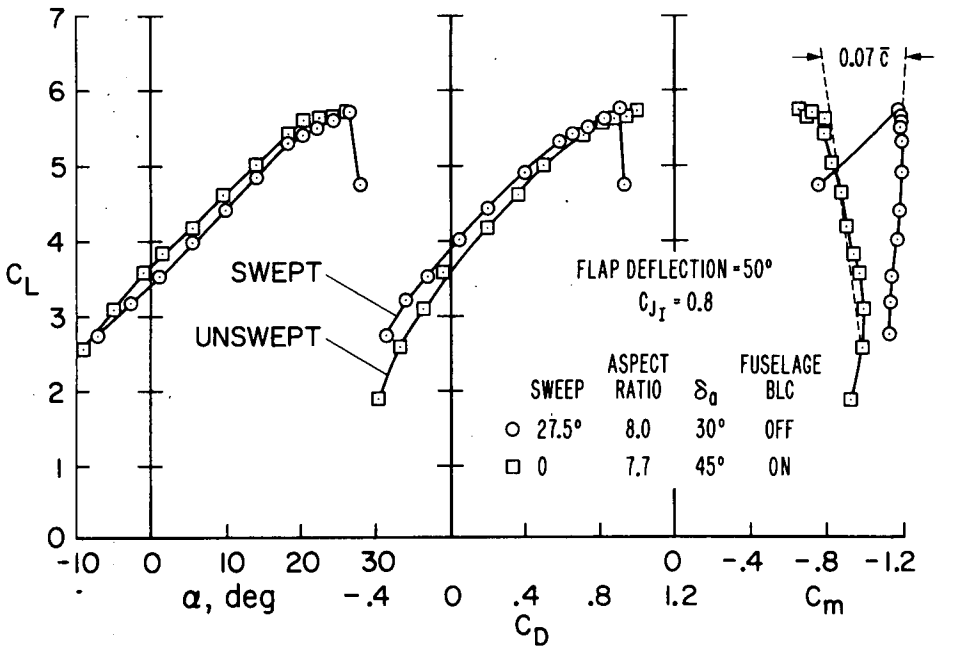

Figure 8

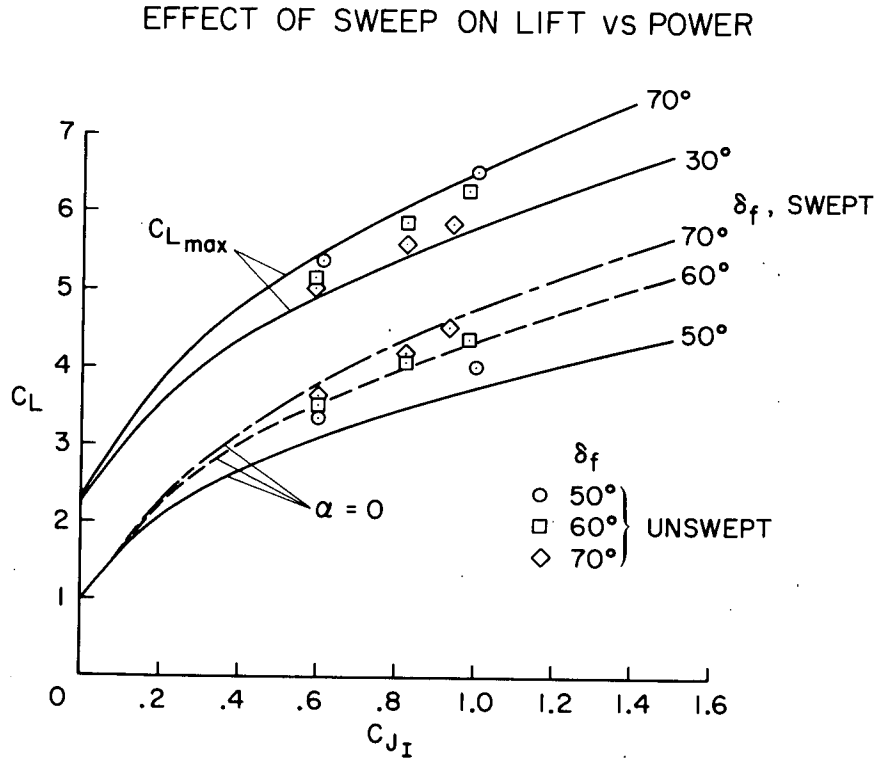

Figure 9

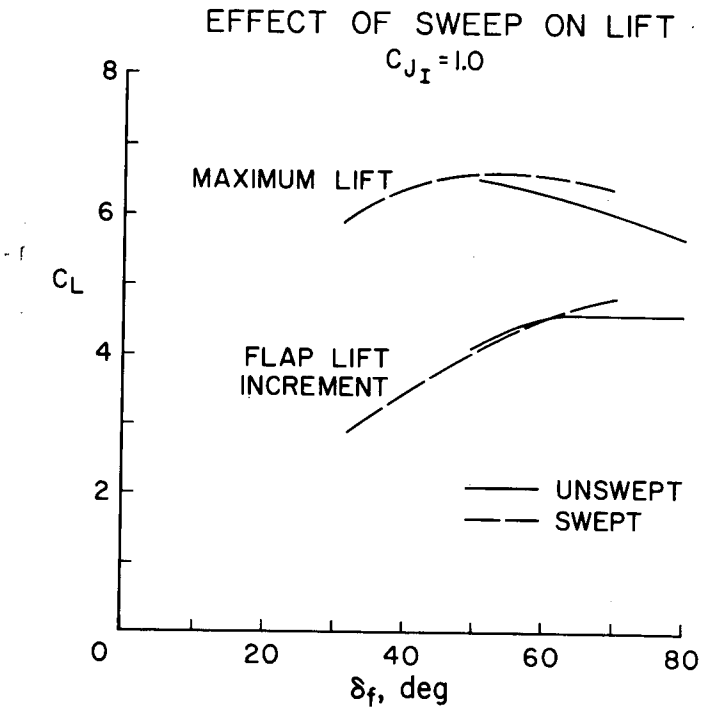

Figure 10

B

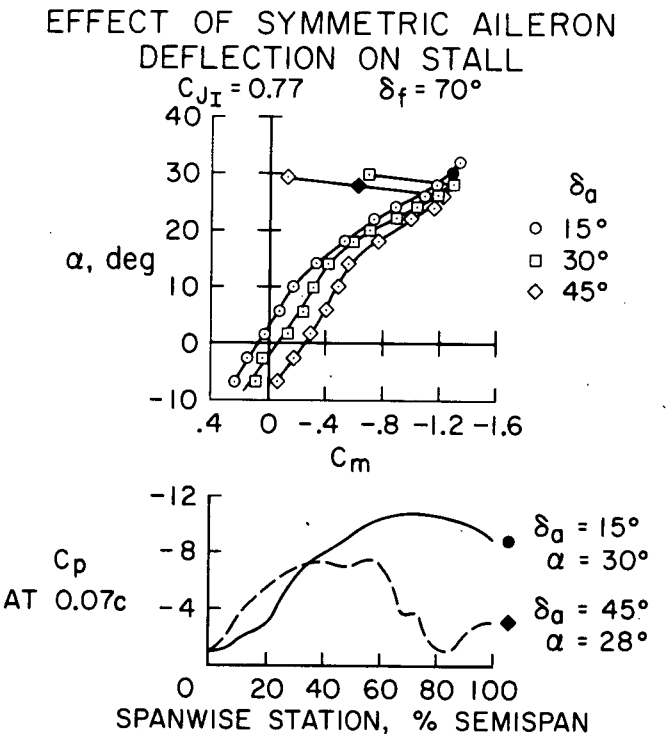

Figure 11

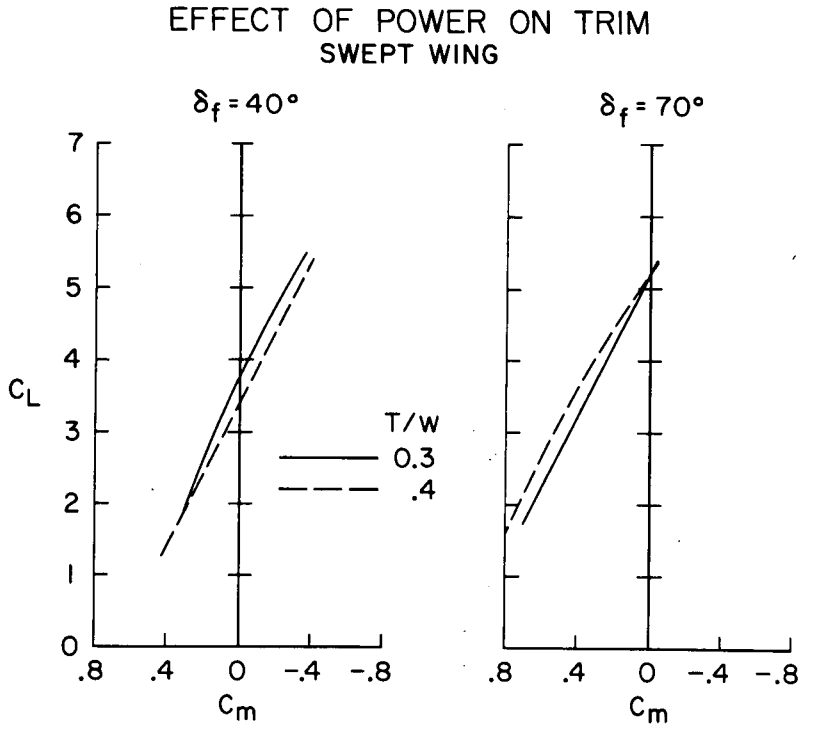

Figure 12

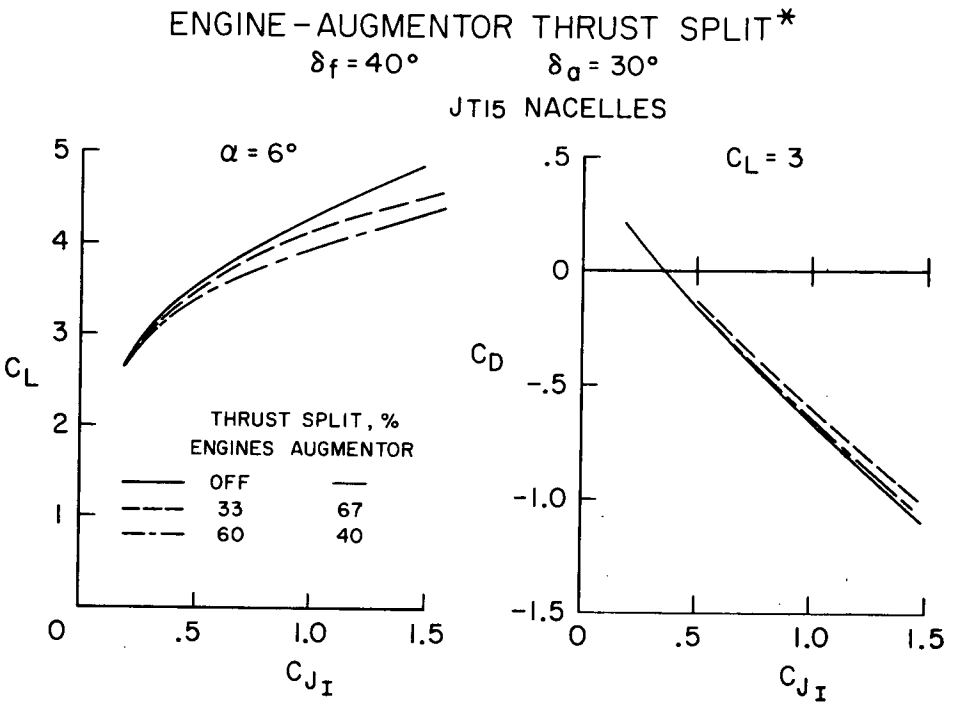

*MEASURED DURING GROUND EFFECT TESTS AT 2.04 CHORDS GROUND HEIGHT

Figure 13

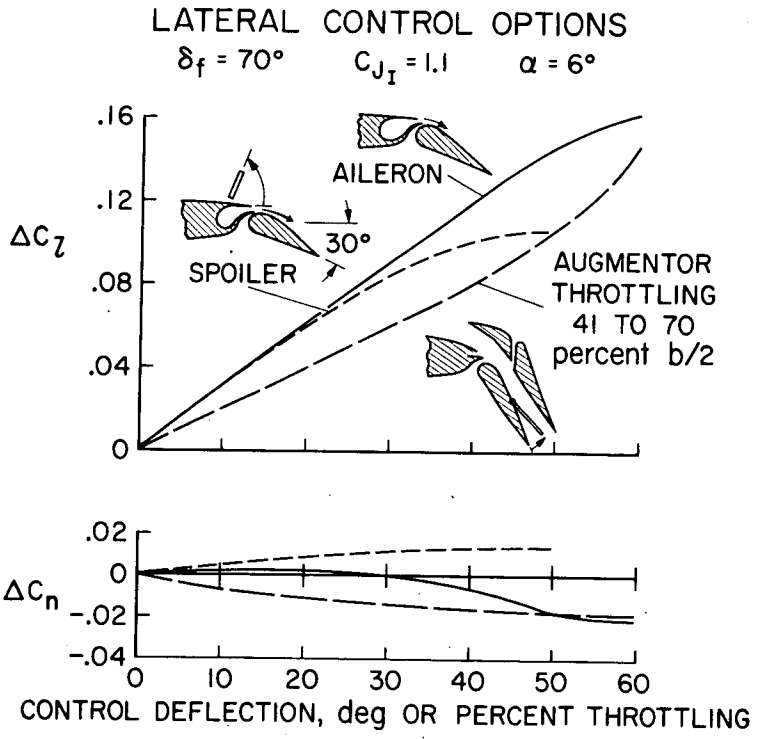

Figure 14

EFFECT OF GROUND HEIGHT

NACELLES OFF

$\delta_f = 70°$

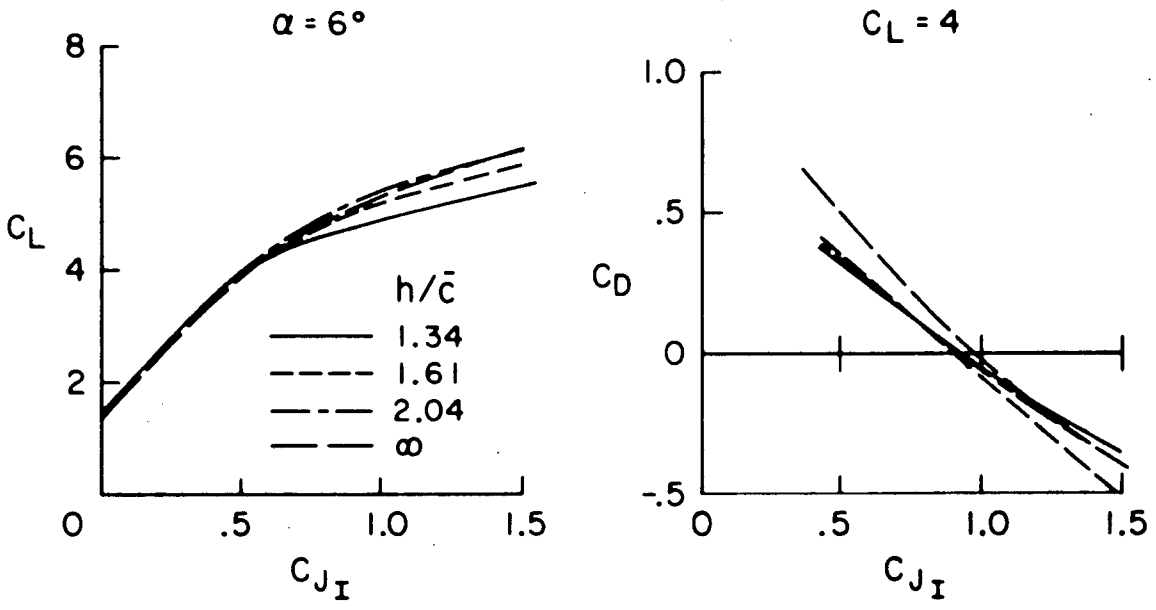

Figure 15

EFFECT OF GROUND HEIGHT

2 J85 NACELLES $\delta_f = 70°$ $\delta_{th} = 60°$

THRUST SPLIT 50:50

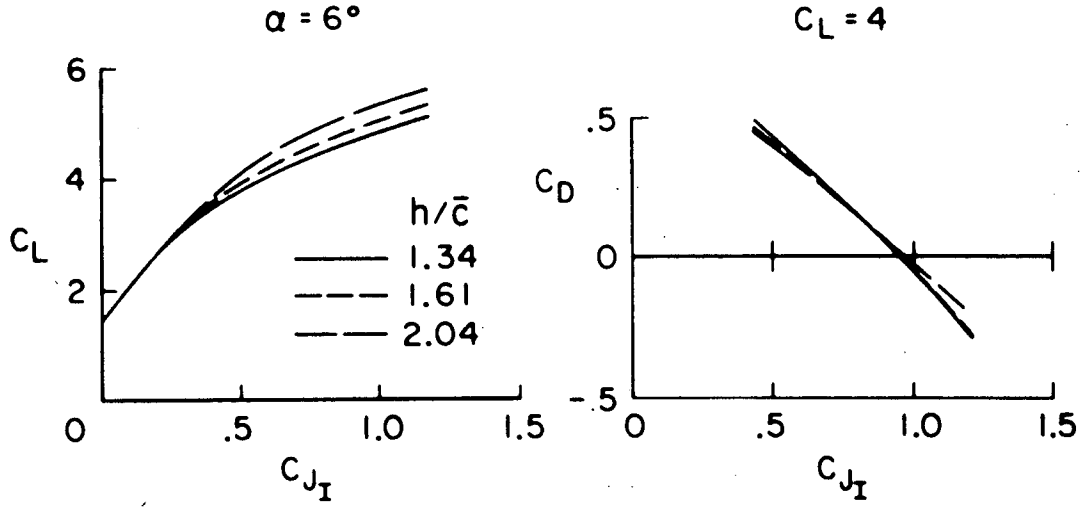

Figure 16